

Low-temperature ionothermal polymerization of phenazine-based small molecules towards ultrastable and high-capacity anode of aqueous alkaline sodium-ion batteries

Xiaorong Yan¹, Mingjun Hu^{1*}, Guoqing Zhao¹, Chuanguang Wu¹, Rui Li², Xinyu Wang², Haiping Yu², Zhihui Wang¹, Bei Wang², Yuxin Hao², Jingru Liu², Yilan Wu^{3*}, Jun Yang^{2,4,*}

1 School of Materials Science and Engineering, Beihang University, Beijing 100191, China

2 Beijing Institute of Nanoenergy & Nanosystems, Chinese Academy of Sciences, Beijing 101400, China

3. School of Chemical Engineering, The University of Queensland, Brisbane, QLD 4072, Australia

4. Shensi Lab, Shenzhen Institute for Advanced Study, University of Electronic Science and Technology of China, Shenzhen 518110, China

*Corresponding authors.

E-mail: mingjunhu@buaa.edu.cn; yilan.wu@uqconnect.edu.au; yangjun@binn.cas.cn.

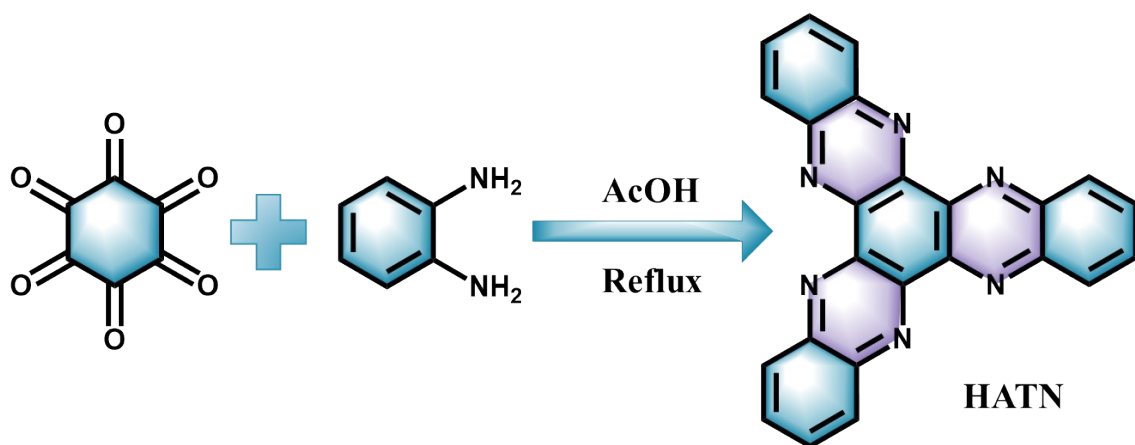


Figure S1. Illustration of the preparation process of HATN.

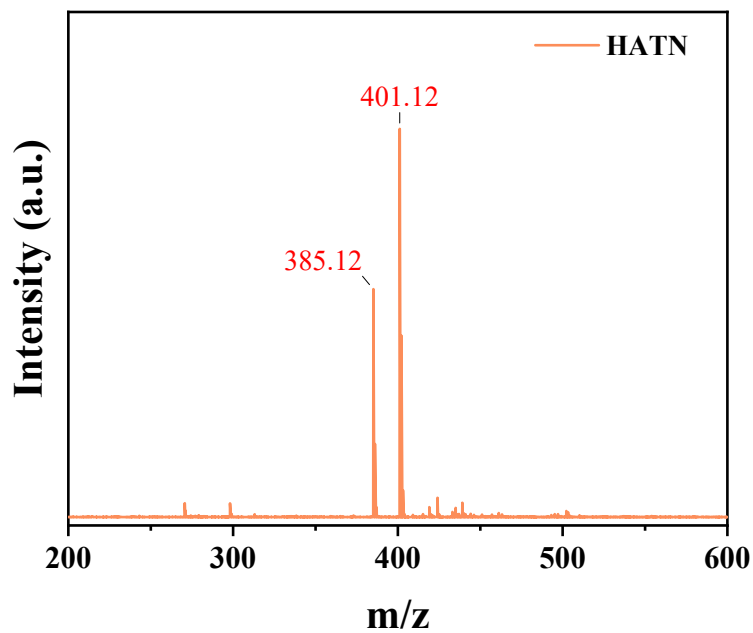


Figure S2. ESI-MS spectrum of HATN. Calculated HATN m/z value: 384, $[HATN+H]^+$: 385, found 385.12, $[HATN+\text{NH}_4]^+$: 401, found 401.12.

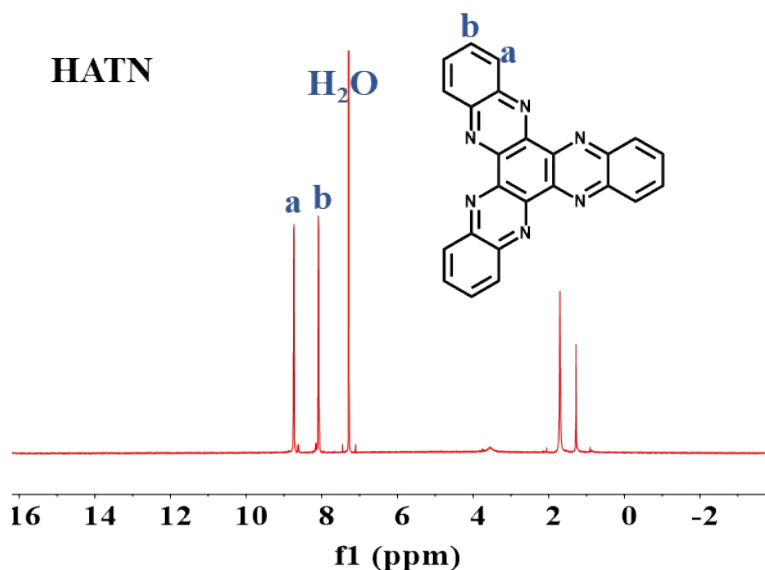


Figure S3. ^1H NMR (400 MHz, CDCl_3) spectrum of HATN.

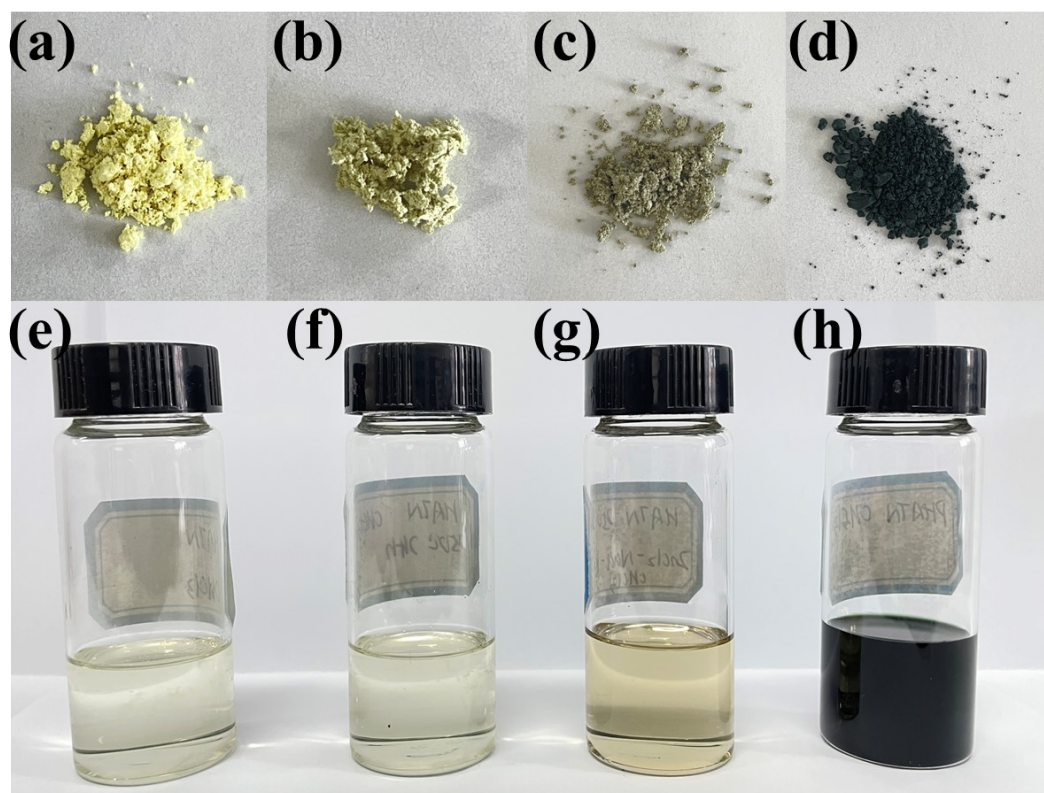


Figure S4. Photographs of products: (a) HATN; (b) the products after heating HATN at 250 °C for 24h; (c) the products after heating the mixture of HATN and ZnCl_2 - NaCl - KCl at 250 °C for 24h; (d) PHATN (the products after heating the mixture of HATN and AlCl_3 - NaCl - KCl at 250 °C for 24h). Photographs to show the solubility of the products in CHCl_3 : (e) the solubility of a; (f) the solubility of b; (h) the solubility of c; (i) the dispersion of d. The results show the PHATN is black and was not well dissolved by CHCl_3 .

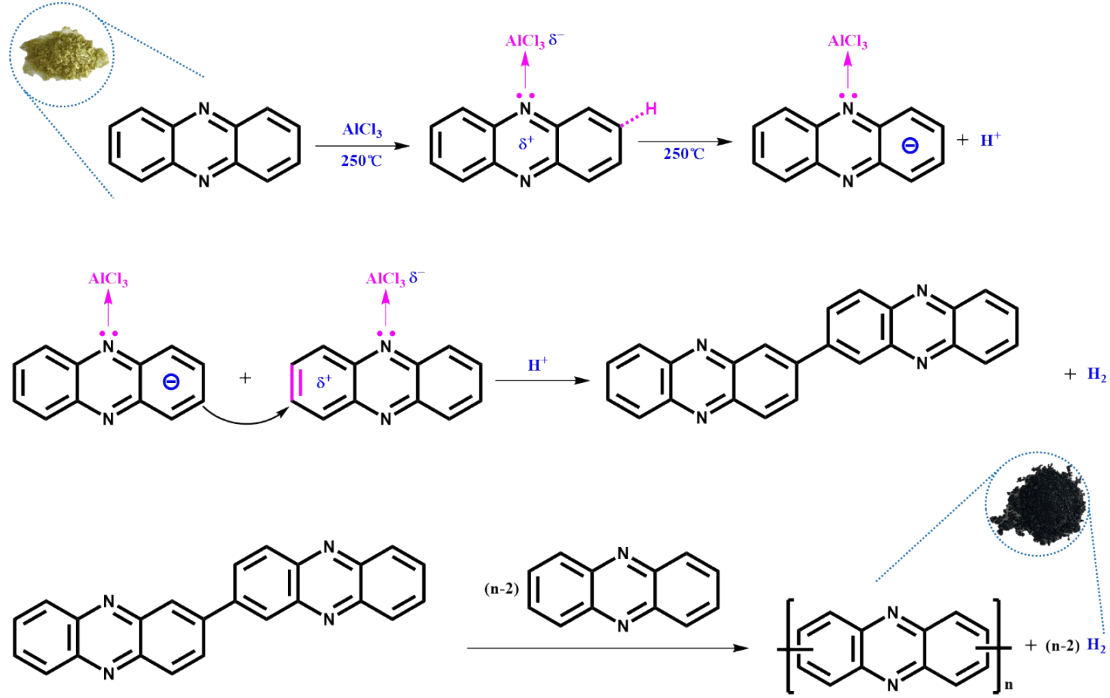


Figure S5. The proposed dehydrocoupling reaction mechanism of PPZ.

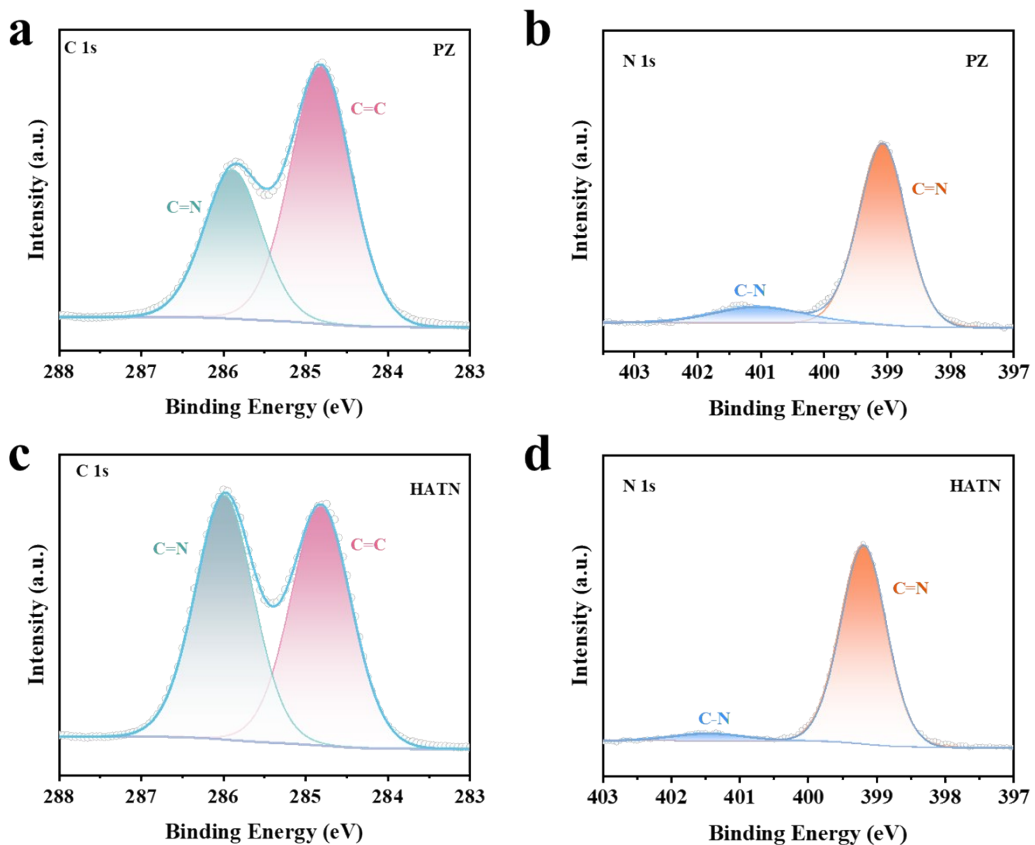


Figure S6. (a) The C 1s XPS spectra of PZ. (b) The N 1s XPS spectra of PZ. (c) The C 1s XPS spectra of HATN. (d) The N 1s XPS spectra of HATN.

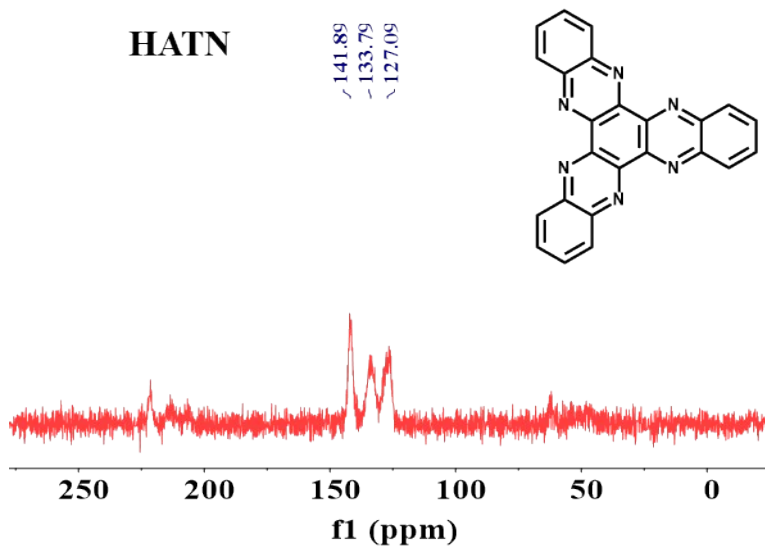


Figure S7. ^{13}C solid-state NMR spectrum of HATN.

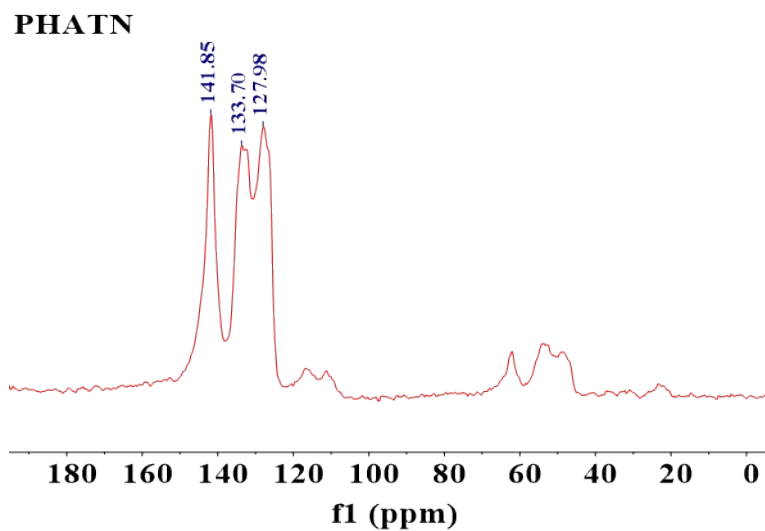


Figure S8. ^{13}C solid-state NMR spectrum of PHATN.

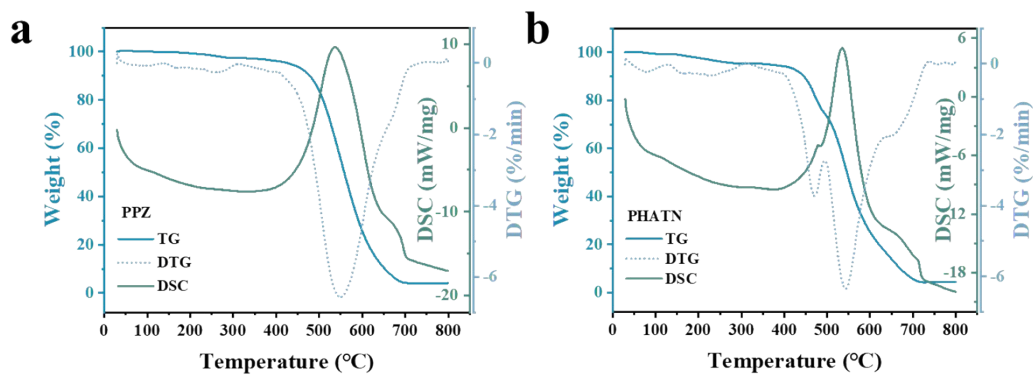


Figure S9. The TGA, DTG and DSC curves of (a) PPZ and (b) PHATN in Air.

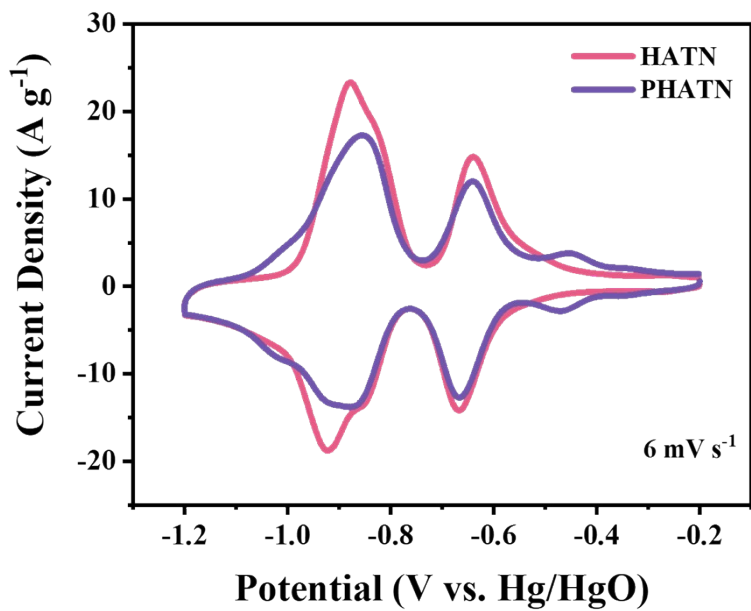


Figure S10. CV curves of HATN and PHATN at 6 mV s^{-1} .

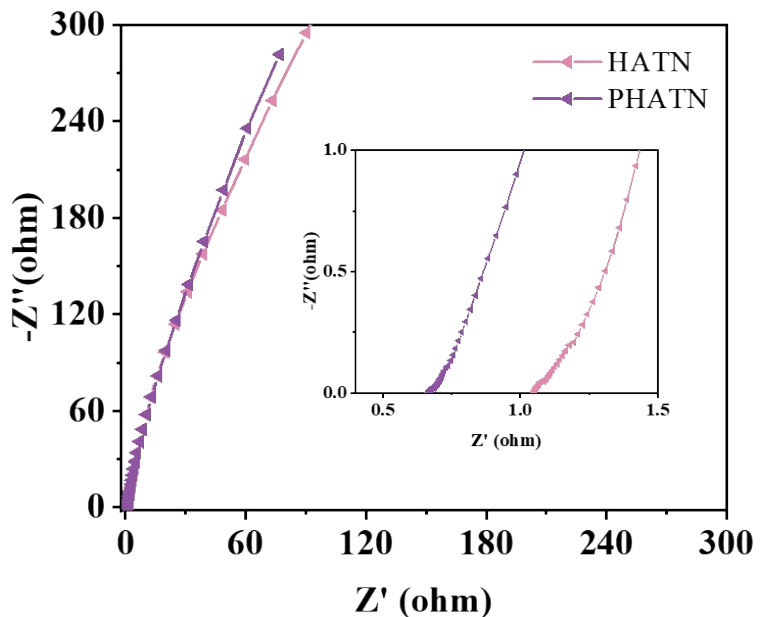


Figure S11. The electrochemical impedance spectrum (EIS) of HATN and PHATN.

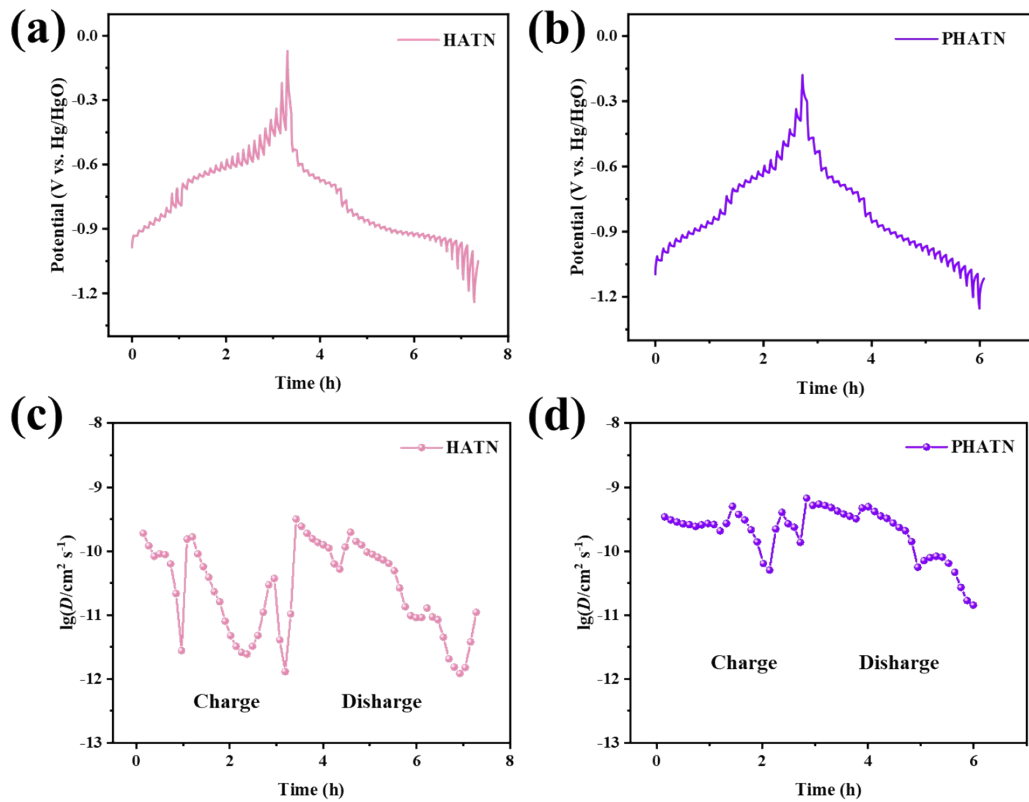


Figure S12. The GITT curves of (a) HATN and (b) PHATN; The ion diffusion coefficients of (c) HATN and (d) PHATN.

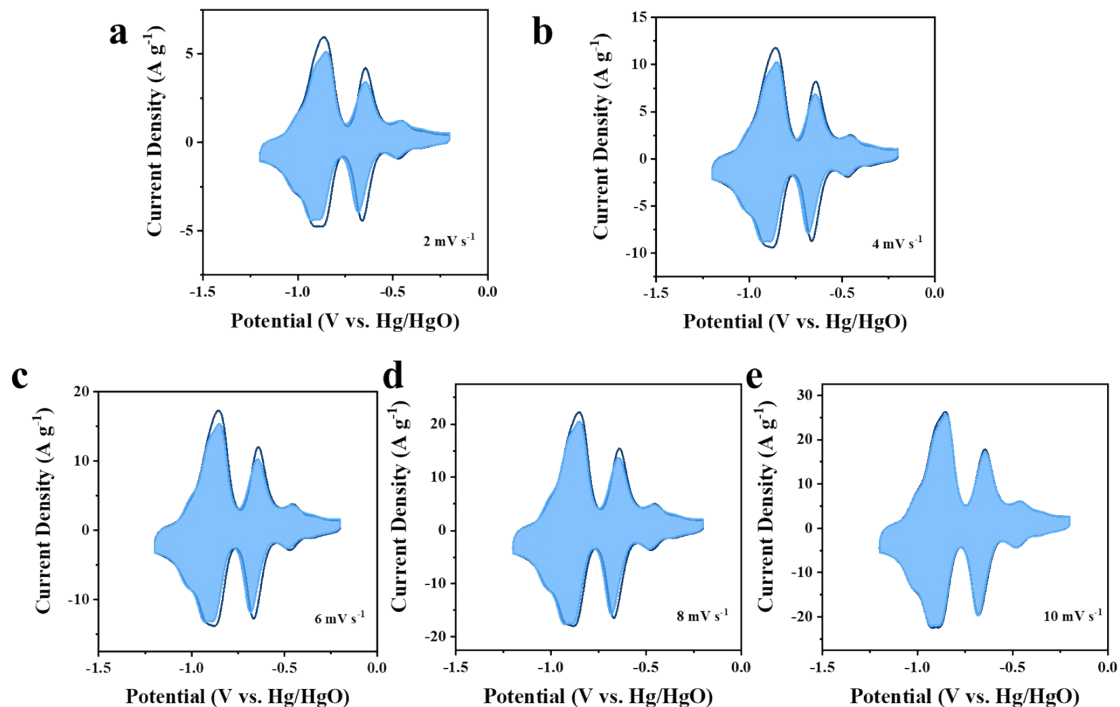


Figure S13. The calculated capacitive current curves (blue regions) at different scan rates (2mV s^{-1} ; 4mV s^{-1} ; 6mV s^{-1} ; 8mV s^{-1} ; 10mV s^{-1}) of PHATN.

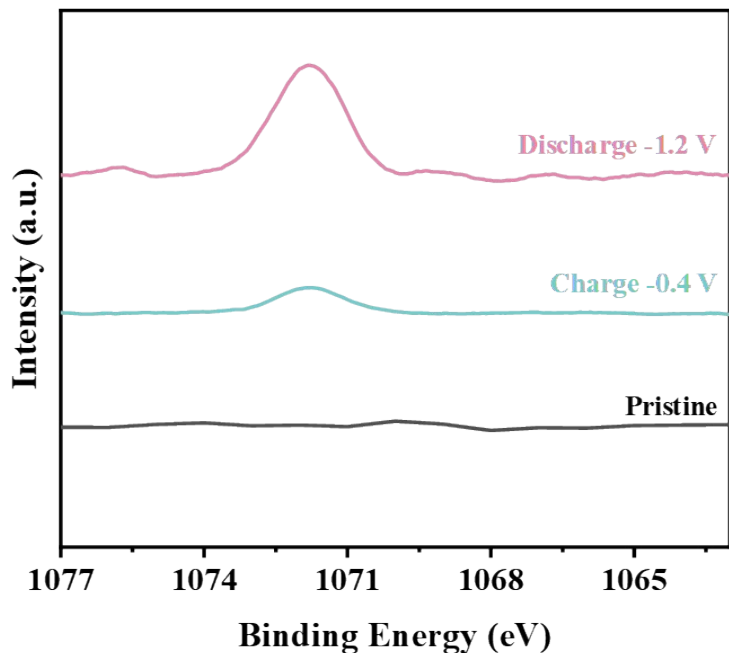


Figure S14. Na 1 s XPS spectra of PHATN at different discharge and charge states.

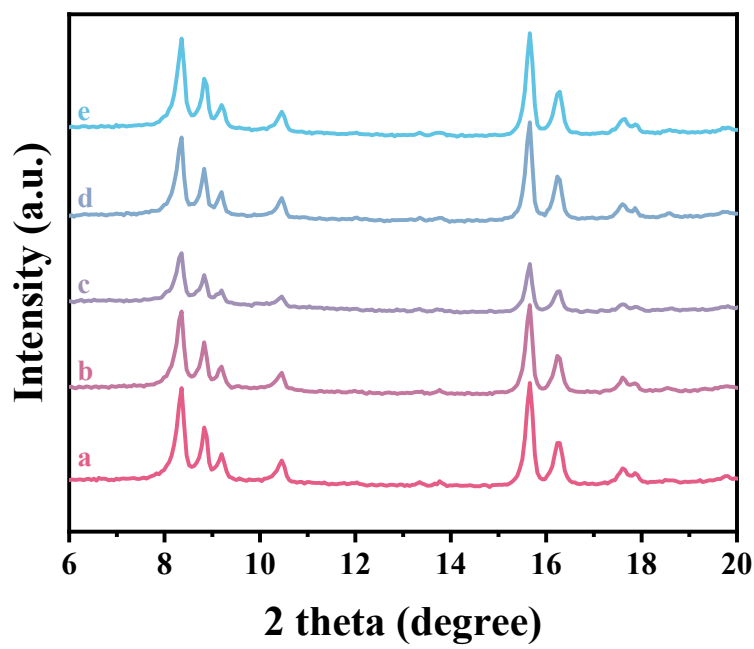


Figure S15. Ex-situ XRD of PHATN electrode as the anode at different discharge and charge states.

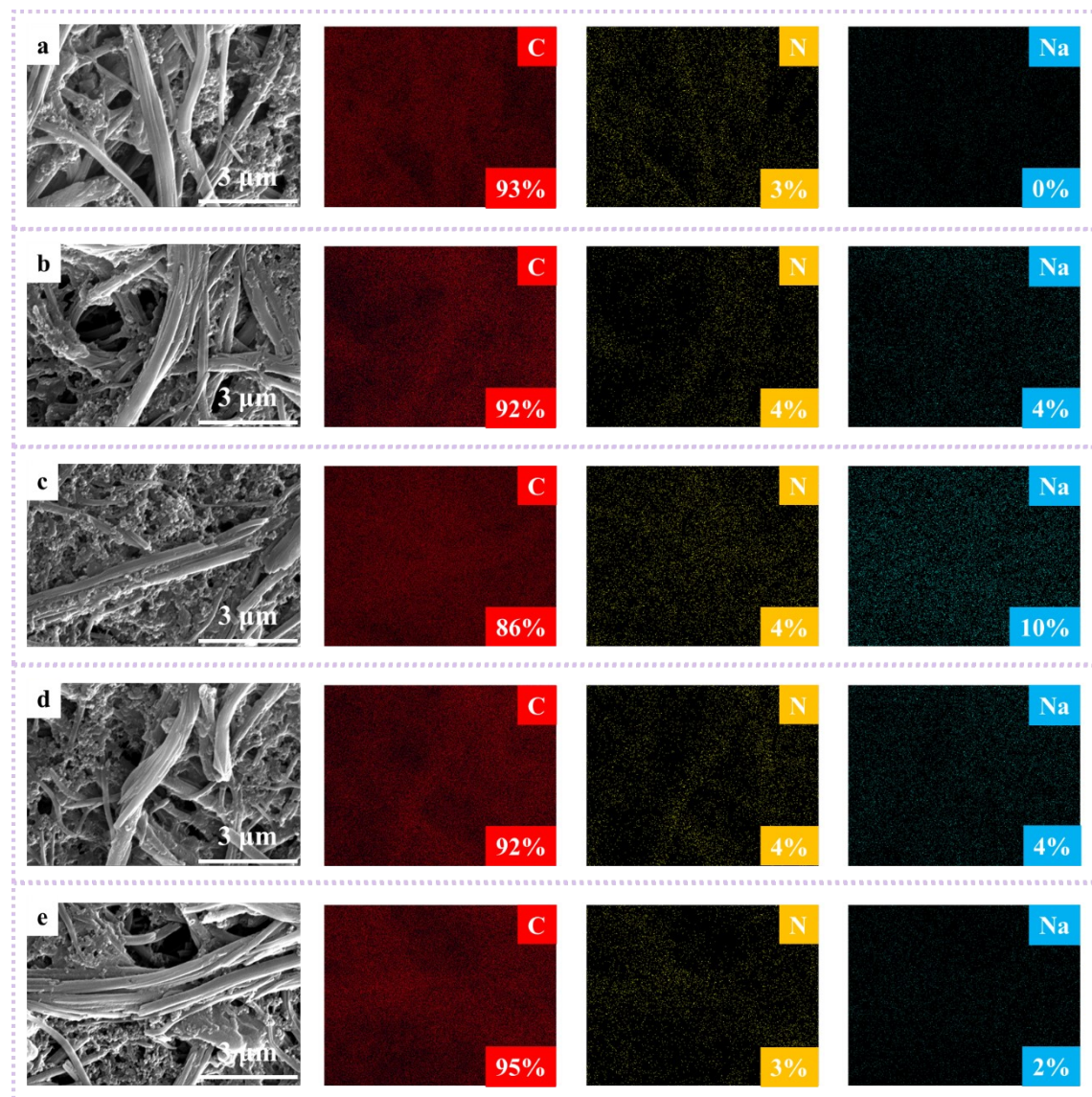


Figure S16. The SEM-EDS mapping images of PHATN electrodes at different charge/discharge states.

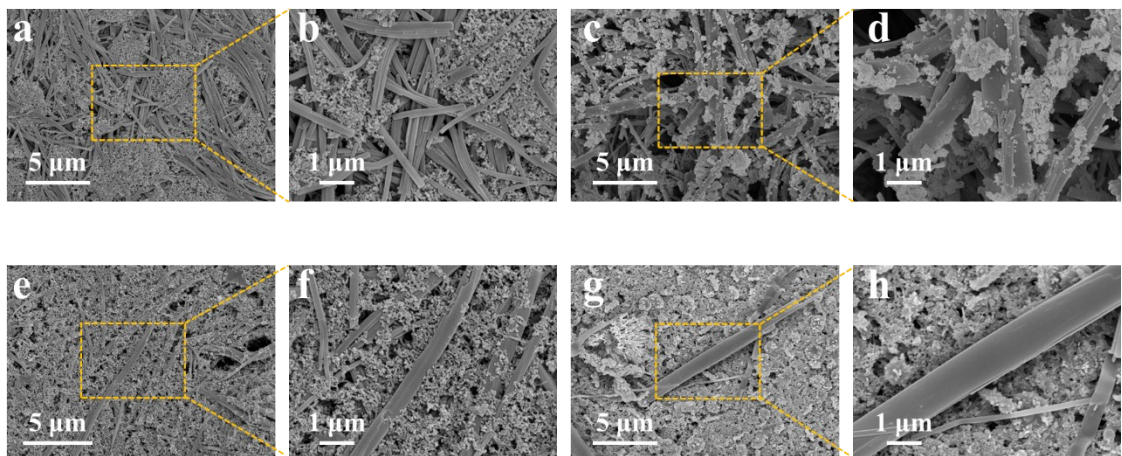


Figure S17. The SEM images of (a, b) pristine electrodes and (c, d) electrodes after 10000 cycles of HATN, and (e, f) pristine electrodes and (g, h) electrodes after 10000 cycles of PHATN.

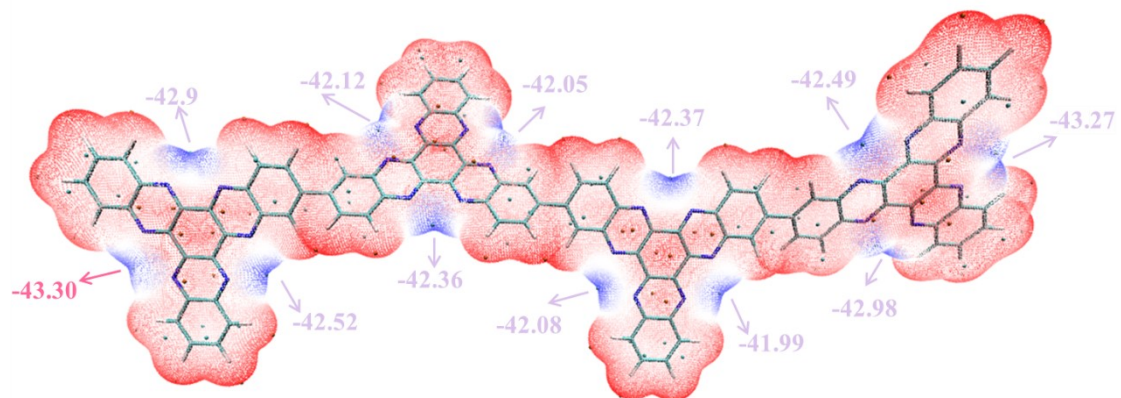


Figure S18. Electrostatic potential diagrams of the tetramer of HATN.

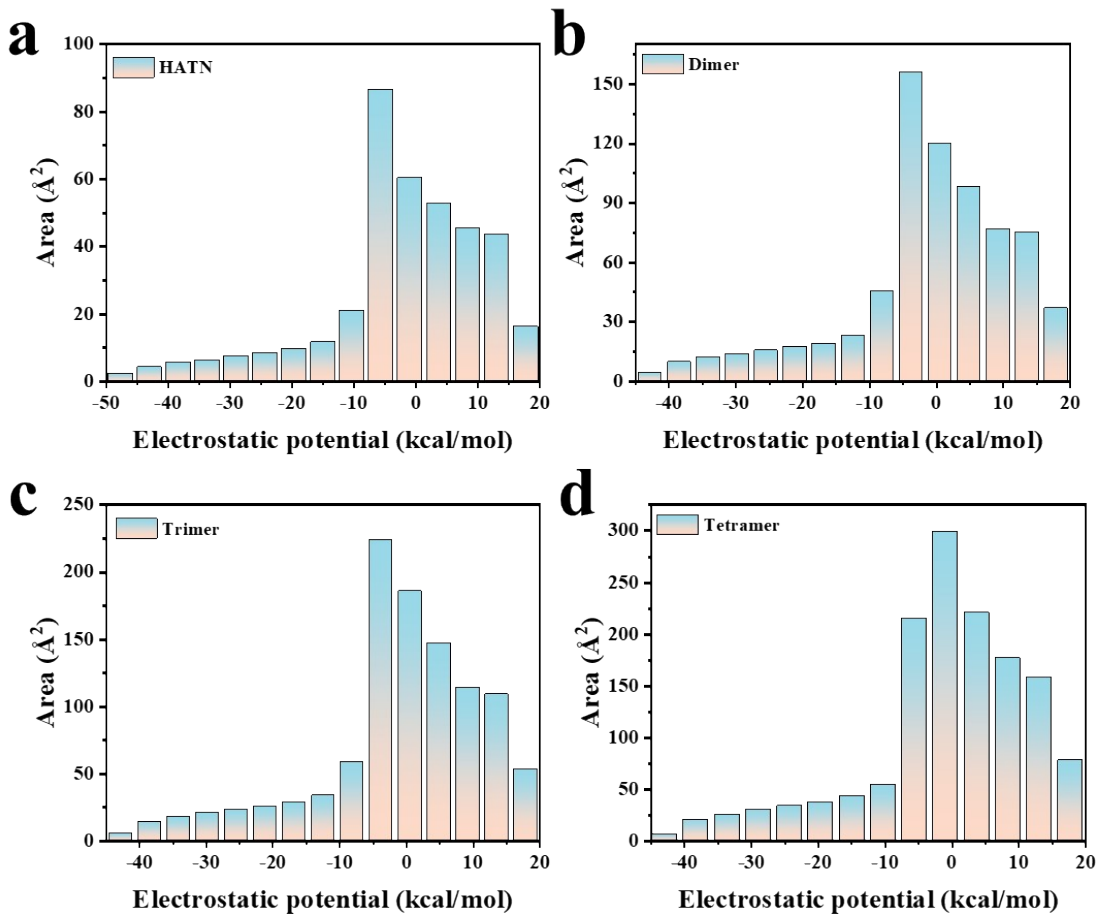


Figure S19. Quantitative distribution of electrostatic potential of HATN, dimer, trimer and tetramer.

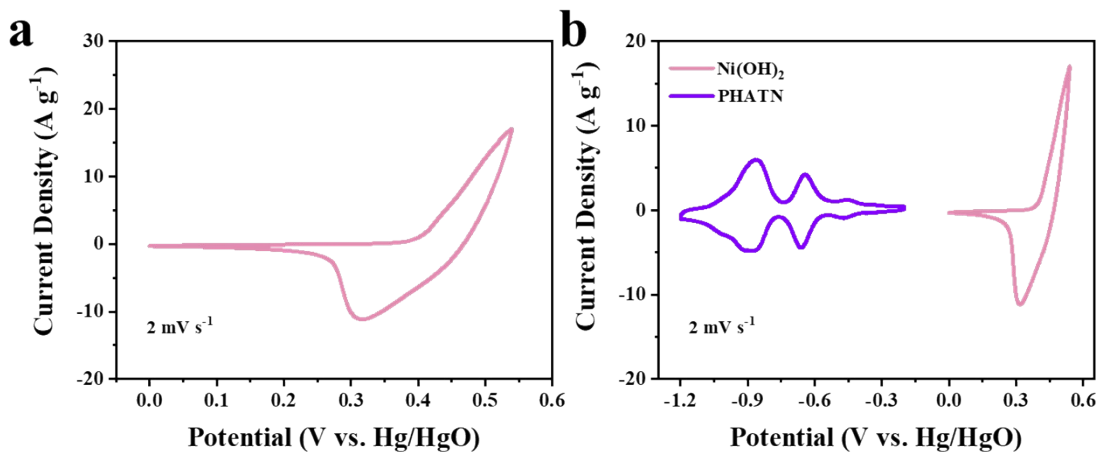


Figure S20. (a) CV curves of Ni(OH)_2 at 2 mV s⁻¹. (b) CV curves of PHATN and Ni(OH)_2 at 2 mV s⁻¹.

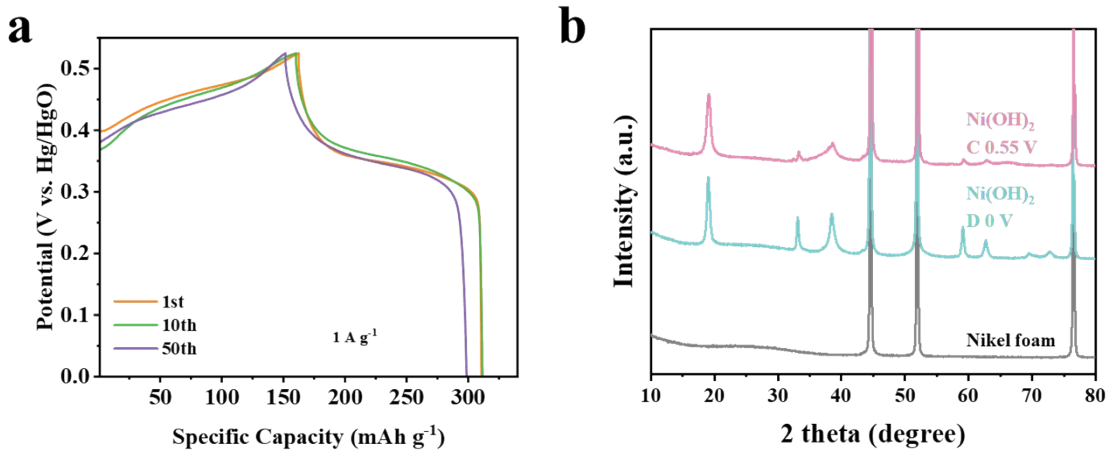


Figure S21. (a) Charge-discharge curves of $\text{Ni}(\text{OH})_2$ electrodes at different cycles. (b) XRD patterns of $\text{Ni}(\text{OH})_2$ electrodes at different charge/discharge states.

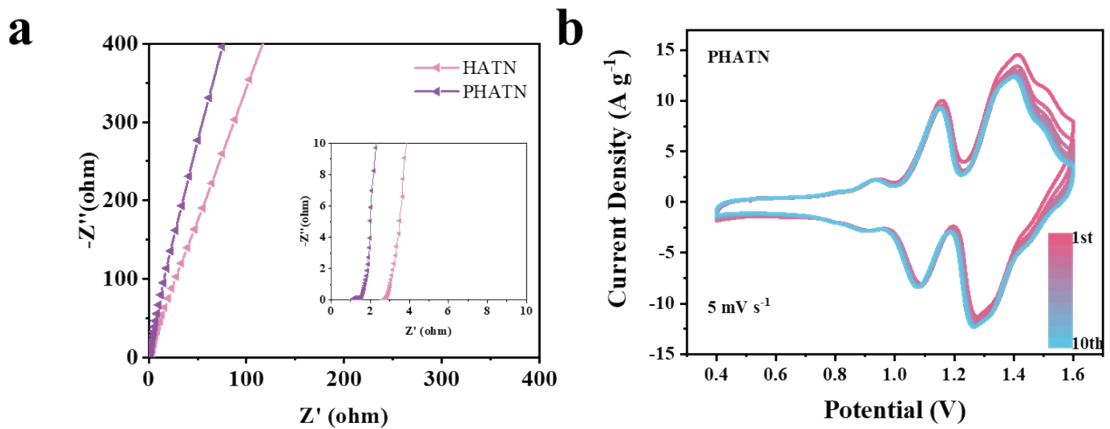


Figure S22. (a) EIS of HATN// $\text{Ni}(\text{OH})_2$ and PHATN// $\text{Ni}(\text{OH})_2$. (b) CV curves of PHATN// $\text{Ni}(\text{OH})_2$ at 5 mV s^{-1} .

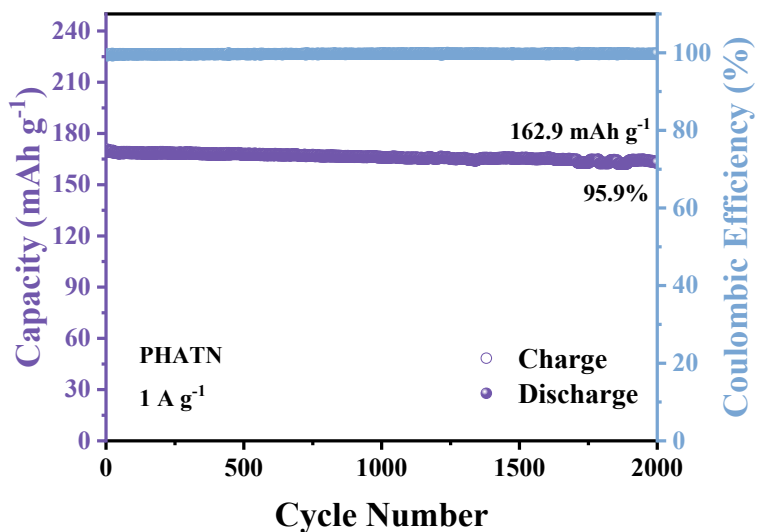


Figure S23. Cycle performance of PHATN// $\text{Ni}(\text{OH})_2$ at 1 A g^{-1} .

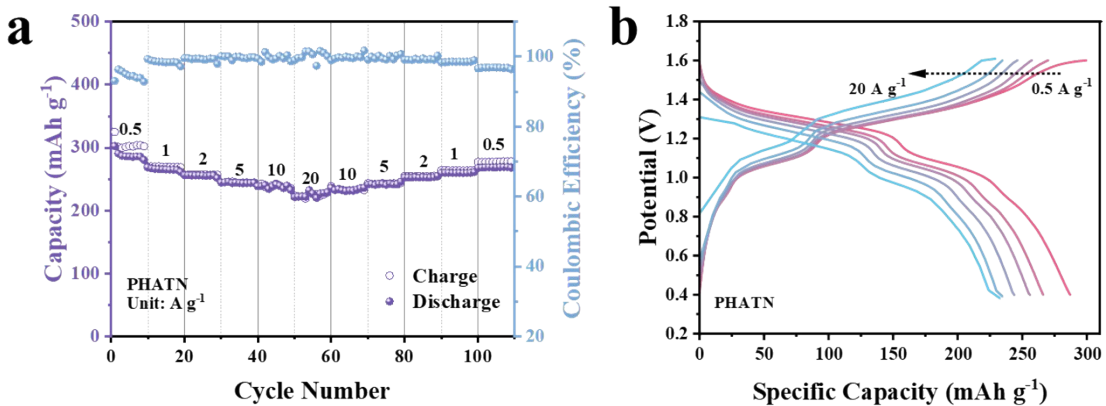


Figure S24. (a) Rate performance and (b) Charge-discharge curves of PHATN//Ni(OH)₂ with the weight ratio of PHATN, ketjen black and PVDF was 3:6:1 at various current densities.

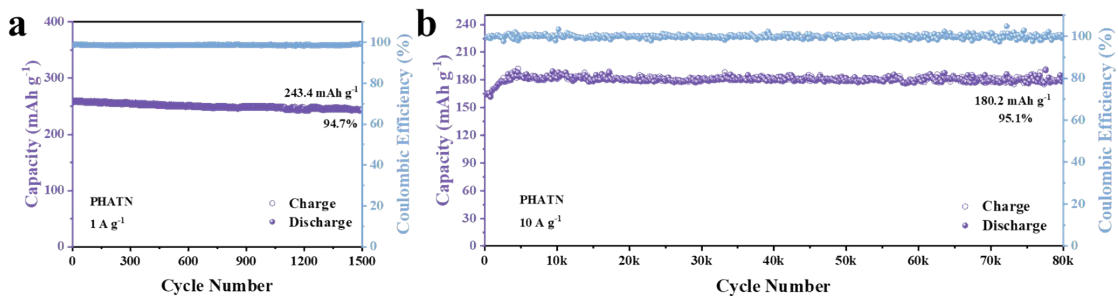


Figure S25. Cycle performance of PHATN//Ni(OH)₂ with the weight ratio of CTF-M, ketjen black and PVDF was 3:6:1 at (a) 1 A g^{-1} and (b) 10 A g^{-1} .

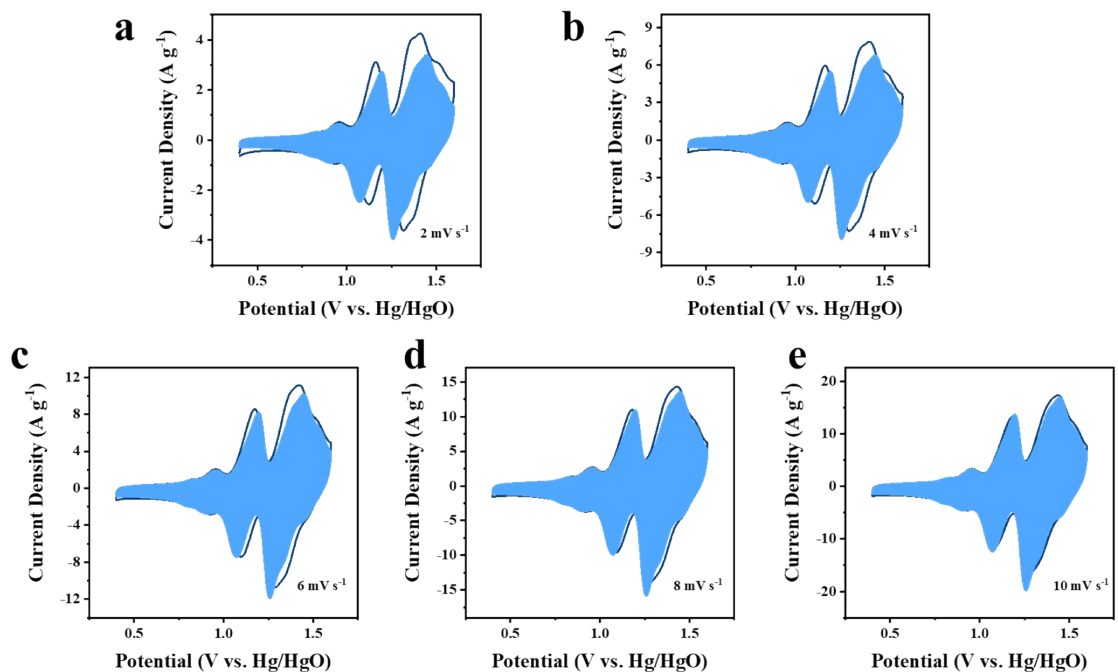


Figure S26. The calculated capacitive current curves (blue regions) at different scan rates (2 mV s^{-1} ; 4 mV s^{-1} ; 6 mV s^{-1} ; 8 mV s^{-1} ; 10 mV s^{-1}) of PHATN//Ni(OH)₂.

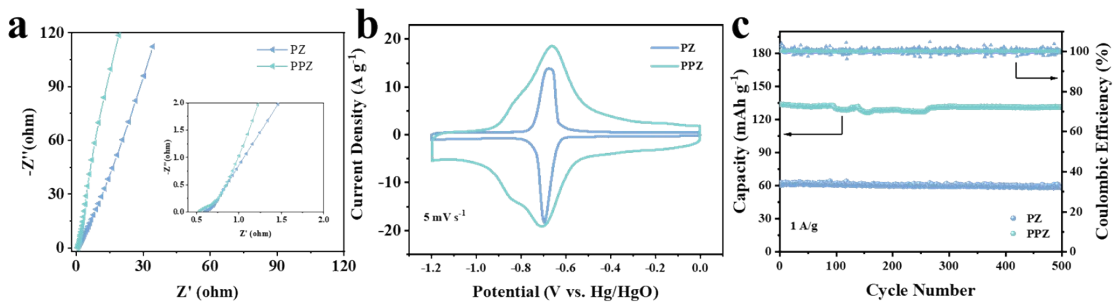


Figure S27. (a) EIS of PZ and PPZ as anode. (b) CV curves of PZ and PPZ as the anode at 5 mV s^{-1} . (c) Cycling performance of PZ and PPZ as anode at 1 A g^{-1}

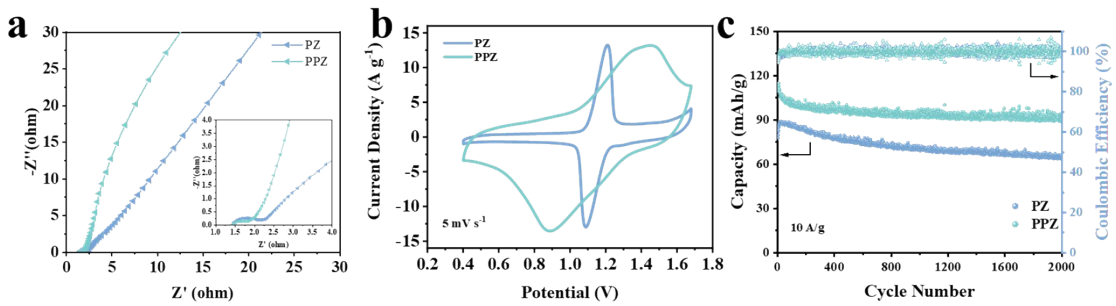


Figure S28. (a) EIS of PZ//Ni(OH)₂ and PPZ//Ni(OH)₂. (b) CV curves of PZ//Ni(OH)₂ and PPZ//Ni(OH)₂ at 5 mV s^{-1} . (c) Cycling performance of PZ//Ni(OH)₂ and PPZ//Ni(OH)₂ at 10 A g^{-1}

Table S1. The electronic conductivity of the obtained samples.

Sample	Test content	Test methods	Results			units
			2 Mpa	4 Mpa	6 Mpa	
PZ	Electrical conductivity	Quadrupole probe	1.39E-07	1.89E-07	2.19E-07	S / m
PPZ	Electrical conductivity	Quadrupole probe	1.33E-04	1.92E-04	2.46E-04	S / m
HATN	Electrical conductivity	Quadrupole probe	2.47E-09	3.82E-09	5.44E-09	S / m
PHATN	Electrical conductivity	Quadrupole probe	1.91E-06	3.60E-06	4.80E-06	S / m

Table S2. Rate performance and cycling performance comparison of PHATN//Ni(OH)₂ with other materials-based aqueous sodium-ion batteries reported in the literature.

Sample	electrolyte	Discharge capacity (mAh g ⁻¹)	Cycling performance (Current density)	Ref.
CDPZ@G // Ni-MOF	10 M NaOH	130.5 (0.5 A g ⁻¹) base on the anode mass	91.3% / After 1500 cycles (6 A g ⁻¹)	1
3CN-DPZ // Ni-BTA	10 M NaOH	323.6 (2 A g ⁻¹) base on the anode mass	96.4% / After 5000 cycles (8 A g ⁻¹)	2
PBA // CrCrPBA	17 M NaClO ₄	52.8 (0.125 A g ⁻¹) base on the anode mass	93.01% / After 500 cycles (3.75 A g ⁻¹)	3
N-NaVTP // N-NaVTP	Saturated NaClO ₄	49.7 (0.2 A g ⁻¹) base on the total mass of cathode and anode	60% / After 1000 cycles (5 A g ⁻¹)	4
Na ₃ MnTi(PO ₄) ₃ // Na ₃ MnTi(PO ₄) ₃	1 M Na ₂ SO ₄	57.9 (0.029 A g ⁻¹) base on the total mass of cathode and anode	98% / After 100 cycles (0.0587 A g ⁻¹)	5
NaTi ₂ (PO ₄) ₃ // Na ₂ NiFe(CN) ₆	0.5 M Na ₂ SO ₄	77 (0.06 A g ⁻¹) base on the total mass of cathode and anode	96% / After 300 cycles (0.06 A g ⁻¹)	6
NaTi ₂ (PO ₄) ₃ // Na ₂ NiFe(CN) ₆	0.5 M Na ₂ SO ₄ // 0.1M Na ₄ Fe(CN) ₆	110 (0.06 A g ⁻¹) base on the total mass of cathode and anode	84.7% / After 1000 cycles (0.09 A g ⁻¹)	6
NaTi ₂ (PO ₄) ₃ // Na ₂ MnFe(CN) ₆	NaClO ₄	61 (0.118 A g ⁻¹) base on the total mass of cathode and anode	74.3% / After 13000 cycles (1.18 A g ⁻¹)	7
LTP@C/CNTs // Na _{0.44} MnO ₂	5 M NaNO ₃	83.36 (0.2 A g ⁻¹) base on the anode mass	79.4% / After 500 cycles (3 A g ⁻¹)	8
NaTi ₂ (PO ₄) ₃ @C// NaVPO ₄ F@C/	17 M NaClO ₄	43.9 (0.1 A g ⁻¹) base on the total mass of cathode and anode	48.8% / After 100 cycles (0.5 A g ⁻¹)	9

Na ₃ V ₂ (PO ₄) ₃ // Na ₃ V ₂ (PO ₄) ₃	NaClO ₄ -H ₂ O-urea ratio of 1-3-2	37 (0.01 A g ⁻¹) base on the total mass of cathode and anode	72% / After 1000 cycles (0.5 A g ⁻¹)	10
NaTi ₂ (PO ₄) ₃ // Na ₃ V ₂ (PO ₄) ₃	NaTFSI: H ₂ O: adiponitrile ratio of 1:1:2.5	96 (0.01 A g ⁻¹) base on the anode mass	71% / After 1000 cycles (0.5 A g ⁻¹)	11
NaTi ₂ (PO ₄) ₃ // Na _{0.44} MnO ₂	NaClO ₄ -H ₂ O-urea ratio of 1-3-2	74.5 (0.02 A g ⁻¹) base on the cathode mass	90% / After 3500 cycles (0.5 A g ⁻¹)	12
NaTi ₂ (PO ₄) ₃ @C// m-NiHCF	5M NaClO ₄	61.4 (0.1 A g ⁻¹) base on the cathode mass	83% / After 600 cycles (0.1 A g ⁻¹)	13
Na ₃ (PO ₄) ₃ // Na ₃ V ₂ (PO ₄) ₃	19 M NaClO ₄ -NaOTF -H ₂ O	40 (0.117 A g ⁻¹) base on the total mass of cathode and anode	87.5% / After 100 cycles (0.117 A g ⁻¹)	14
NaTi ₂ (PO ₄) ₃ // KMnHCF	Polyethylene glycol: H ₂ O ratio of 92:8	105 (0.1 A g ⁻¹) base on the cathode mass	80% / After 3500 cycles (0.8 A g ⁻¹)	15
NaTi ₂ (PO ₄) ₃ @C// HEPBA	1 M Na ₂ SO ₄	75 (0.05 A g ⁻¹) base on the cathode mass	87% / After 1000 cycles (0.1 A g ⁻¹)	16
NaTi ₂ (PO ₄) ₃ // Na ₂ Zn ₃ [Fe(CN) ₆] ₂	17 M NaClO ₄	55 (0.12 A g ⁻¹) base on the cathode mass	100% / After 1000 cycles (0.6 A g ⁻¹)	17
FeHCF // CuHCF	Saturated NaNO ₃	50 (0.06 A g ⁻¹) base on the cathode mass	86% / After 250 cycles (0.3 A g ⁻¹)	18
NaTi ₂ (PO ₄) ₃ -C // AC	1 M Na ₂ SO ₄	100 (0.1 A g ⁻¹) base on the anode mass	61% / After 500 cycles (0.2 A g ⁻¹)	19
Na ₂ VTi(PO ₄) ₃ /C / Na ₂ VTi(PO ₄) ₃ /C	1 M Na ₂ SO ₄	55 (0.05 A g ⁻¹) base on the cathode mass	83% / After 600 cycles (0.4 A g ⁻¹)	20
PHATN // Ni(OH) ₂	6 M NaOH	302.5 (0.5 A g ⁻¹) base on the anode mass	95.1% / After 80000 cycles (10 A g ⁻¹)	This work

Notes and references

- 1 J. He, R. Wang, L. Li, L. Zhao, M. Shi and C. Yan, *Chem Commun*, 2022, **58**, 11925–11928.
- 2 R. Wang, M. Shi, L. Li, Y. Zhao, L. Zhao and C. Yan, *Chemical Engineering Journal*, 2023, **451**, 138652.
- 3 J. Chen, C. Liu, Z. Yu, J. Qu, C. Wang, L. Lai, L. Wei and Y. Chen, *Chem Eng J*, 2021, **415**, 129003.
- 4 Q. Y. Meng, J. C. Shao, X. R. Dou and H. Z. Chi, *Small*, **20**, 2308483.
- 5 H. Gao and J. B. Goodenough, *Angewandte Chemie International Edition*, 2016, **55**, 12768–12772.
- 6 W. Zhou, Y. Zheng, M. Zartashia, Y. Shan, H. Noor, H. Lou and X. Hou, *Acs Appl Mater Inter*, 2022, **14**, 34835–34843.
- 7 H. Wu, J. Hao, Y. Jiang, Y. Jiao, J. Liu, X. Xu, K. Davey, C. Wang and S.-Z. Qiao, *Nat Commun*, 2024, **15**, 575.
- 8 T. Xu, M. Zhao, Z. Su, W. Duan, Y. Shi, Z. Li, V. G. Pol and X. Song, *Journal of Power Sources*, 2021, **481**, 229110.
- 9 Y. Wang, D. Bin, C. Wang, Y. Cao and Y. Xia, *Batteries & Supercaps*, 2023, **6**, e202300275.
- 10 Z. Hou, M. Dong, Y. Xiong, X. Zhang, Y. Zhu and Y. Qian, *Advanced Energy Materials*, 2020, **10**, 1903665.
- 11 H. Wang, T. Liu, X. Du, J. Wang, Y. Yang, H. Qiu, G. Lu, H. Li, Z. Chen, J. Zhao and G. Cui, *Batteries Supercaps*, 2022, **5**, e202200246.
- 12 Z. Hou, X. Zhang, J. Chen, Y. Qian, L.-F. Chen and P. S. Lee, *Advanced Energy Materials*, 2022, **12**, 2104053.
- 13 L. Shen, Y. Jiang, Y. Liu, J. Ma, T. Sun and N. Zhu, *Chemical Engineering Journal*, 2020, **388**, 124228.
- 14 T. Jin, X. Ji, P.-F. Wang, K. Zhu, J. Zhang, L. Cao, L. Chen, C. Cui, T. Deng, S. Liu, N. Piao, Y. Liu, C. Shen, K. Xie, L. Jiao and C. Wang, *Angewandte Chemie*

- International Edition*, 2021, **60**, 11943–11948.
- 15J. Liu, C. Yang, B. Wen, B. Li and Y. Liu, *Small*, 2023, **19**, 2370387.
- 16X. Zhao, Z. Xing and C. Huang, *J. Mater. Chem. A*, 2023, **11**, 22835–22844.
- 17M. Shao, B. Wang, M. Liu, C. Wu, F.-S. Ke, X. Ai, H. Yang and J. Qian, *Acs Appl Energ Mater*, 2019, **2**, 5809–5815.
- 18B. Wang, X. Wang, C. Liang, M. Yan and Y. Jiang, *ChemElectroChem*, 2019, **6**, 4848–4853.
- 19X. Cao and Y. Yang, *Mater Lett*, 2018, **231**, 183–186.
- 20J. Dong, G. Zhang, X. Wang, S. Zhang and C. Deng, *J. Mater. Chem. A*, 2017, **5**, 18725–18736.